Online Only Supplementary Section for:

High Intensity Interval Training in Aged Female Mice Prevents Frailty and Preserves Physical, Cognitive, and Cardiovascular Function

Drew Theobald[1], Phillip Williamson[2], Alexandra Johnston[1], Lucas Tripp[2], Ayodeji A. Olabiyi[3], Xavier Silvers[4], Tuan D. Tran[5], Lisandra de Castro Braz[3], Srinivas Sriramula[1],Ted G. Graber[2,3,4,#]

Affiliations: East Carolina University (ECU), [1] Dept. of Pharmacology, [2] Dept. of Physical Therapy, [3] Dept. of Physiology, [4] Dept. of Kinesiology, [5] Dept. of Psychology

[#] Corresponding/Senior Author: Ted G. Graber, PhD
Assistant Professor
East Carolina University
Dept. of Physical Therapy
Email: grabert19@ecu.edu

Table of Contents

Supplemental Methods

In vivo Outcome Measures:

Body Composition: We measured body mass weekly and body composition (with EchoMRI) pre- and post-intervention. We have previously detailed EchoMRI, which we use to report lean mass and fat percentage changes.(1-2)

Blood pressure measurement: Blood pressure was measured using noninvasive tail-cuff plethysmography according to the manufacturer's protocol (CODA Kent Scientific). Prior to baseline blood pressure measurements, mice were acclimatized to the procedure for 5 consecutive days. All experiments were performed in a designated quiet area at the same time each day. Mice were guided into appropriately sized restraint tubes, and nose cones were adjusted to minimize movement. Heating platforms were used to maintain a body temperature of 32°-35°C before and throughout recordings. Occlusion and Volume Pressure Recording (VPR) cuffs were inspected for leaks prior to each session. The occlusion cuff was positioned at the base of the tail with the VPR sensor placed directly behind it. The occlusion cuff was inflated and deflated over 20 s while the VPR sensor detected changes in the tail volume during blood return. The minimum tail volume was set to 15 µL. Mice underwent 5 acclimation cycles followed by 25 measurement cycles with an 8 s interval between cycles. At least 5 accepted values from the measurement cycles were used for analysis. Blood pressure was recorded for three consecutive days each week, and the values were averaged to obtain one weekly measurement for each mouse.

Echocardiography imaging: Echocardiography imaging is a non-invasive procedure that allows assessment of both systolic and diastolic function. Echocardiography was performed twice for each animal; before training and after training, in both the HIIT and SED groups. Examinations were performed using a digital ultrasonic imaging system (Vevo 3100, Fujifilm VisualSonics, USA). Briefly, mice were initially anesthetized by placing them in a flow-through system containing approximately 2-3.5% isoflurane in 100% oxygen. Following loss of consciousness, mice were placed on a modified mask assembly that allowed continuous delivery of approximately 1-2.5% isoflurane in oxygen. The mice breathed spontaneously, and the depth of anesthesia was monitored by the operator and through continuous recording of heart rate. It was crucial to maintain heart rate above 400 beats/min, as the accuracy of the images obtained depends on a near physiological heart rate. Mice were acclimatized for ~5 min on an isothermal pad to maintain body temperature, and then hair was removed where needed before images were recorded as described previously and according to the Guidelines for Measuring Cardiac Physiology in Mice.(3-5)

Whole Body Metabolism: Promethion Metabolic Chambers (Sable Systems) were used with the manufacturer's instructions at a 12-hour/12-hour light/dark cycle held at a constant 23°C for 6 or 7 days. Both the running wheels and the laser x/y/z plane activity grids were active to measure voluntary wheel running and activity rate, respectively and adjusted to meters per day (m/day). We report whole body calorimetry (vO2, oxygen consumption, vCO2, carbon dioxide production, RER, respiratory exchange ratio, and kilocalories per hour expended, Kcal/hr) as the overall mean and the maximum number recorded. Food and water consumption, and body mass, were recorded throughout the length of the procedure (data not shown).

Ex vivo Outcome Measures:

Immunohistochemistry: Brain and heart tissues were collected from anesthetized mice and post-fixed in 4% paraformaldehyde in 0.1 M phosphate-buffered saline (PBS; pH 7.4), followed by cryoprotection in 30% sucrose in PBS overnight. Brains were sectioned coronally at 25 µm using an HM 430 sliding microtome. Hearts were paraffin embedded and sagittally sectioned at 5 µm onto glass slides. Paraffin sections were deparaffinized and subjected to heat-induced antigen retrieval. Immunofluorescence staining was performed, as previously described.(27) Briefly, free-floating brain sections and heart sections were washed in 1× PBS and incubated for 1 h at room temperature in blocking solution containing 2% normal donkey serum, 0.05% Tween-20, 50 mM glycine, 0.1% Triton X-100, 0.1% bovine serum albumin, and 1x PBS. Sections were then incubated overnight at 4 °C in a humidified chamber with the following primary antibodies: connexin 43 (Cx43; Sigma-Aldrich C6219, 1:500), α-smooth muscle actin (αSMA; Novus NB300-978, 1:500), glial fibrillary acidic protein (GFAP; Invitrogen 14-9892-2, 1:500), AIF1/IBA1 (ABclonal A19776, 1:1000), and interleukin-1β (IL-1β; Invitrogen P420B, 1:500). Following washes in PBS containing 0.5% Tween-20, sections were incubated for 2 h at room temperature with the appropriate Alexa Fluor conjugated secondary antibodies (Invitrogen A32794, A32849, A32816, A32795; all 1:1000). Sections were mounted using VECTASHIELD antifade mounting medium with DAPI (Vector Laboratories, H-1800). For all brain analyses, anatomically matched sections of the hippocampal CA1 region were used, as it is particularly vulnerable to age-associated neuroinflammatory remodeling and plays a central role in learning and memory. Cardiac analyses were performed in the left ventricle as this region is highly associated with hypertrophy, fibrosis, and extracellular matrix remodeling. A minimum of five images per section were captured using a fluorescence microscope. Mean fluorescence intensity was quantified using ImageJ software (NIH). Representative images were selected from samples whose quantified values were closest to the group mean to best reflect the average response.

Cardiomyocyte Cross-Sectional Area: For cardiomyocyte cross-sectional area analysis, cell membranes were labeled with wheat germ agglutinin (WGA) conjugated to Alexa Fluor 488 (Invitrogen W11261; 1 mg/mL stock, 1:200 dilution) for 10 min as previously described.(6,7) Sections were mounted with VECTASHIELD antifade mounting medium with DAPI. Images were acquired using a fluorescence microscope (Keyence/Echo Revolve). Cardiomyocyte cross-sectional area in the left ventricle was quantified in ImageJ by a blinded investigator.

Measurement of Collagen: To determine the extent of collagen deposition as a measure of cardiac remodeling, heart tissue sections were stained with 0.1% Picrosirius Red to visualize fibrillar collagen as previously described.(3) Sections were imaged under standard brightfield microscopy by an investigator blinded to the experimental groups. Collagen-positive staining in the left ventricular myocardium was quantified using identical thresholding parameters across all groups.

Microglial Morphological Analysis: To quantify microglial reactivity, AIF1/IBA1-labeled images from the CA1 region were acquired at 63x magnification using a confocal microscope. Microglial morphology was analyzed using the AnalyzeSkeleton (2D/3D) plugin in Fiji/ImageJ, as previously described, images were converted to 8-bit grayscale, and brightness and contrast were adjusted using the maximum slider to visualize microglial processes.(6) Contrast was further enhanced using the Unsharp Mask tool (pixel radius: 3; mask weight: 0.6), followed by despeckling to reduce noise. Images were converted to binary, skeletonized, and analyzed to quantify average length and number of branches.

Astrocyte Ramification Analysis: Astrocyte complexity in the hippocampal CA1 region was quantified using the Shoenen ramification index, defined as the ratio of the maximum number of

Sholl intersections to the number of primary branches. Images were imported into Fiji and analyzed using the Simple Neurite Tracer (SNT) plugin. Astrocytes were reconstructed according to the Fiji SNT walkthrough protocol (https://imagej.net/plugins/snt/walkthroughs), with the starting point defined as the center of DAPI staining and all primary processes traced outward. Sholl analysis was performed using the Fiji SNT Sholl protocol (https://imagej.net/plugins/snt/sholl) at a radius step size of 4 μm.

Soleus (SOL) Muscle Morphology: As previously described, we used immunofluorescence to test for fiber type distribution (myosin heavy chain 1, MHC1, MHC2a, MHC2x, and hybrid fibers) and cross-sectional area by fiber type in a randomly selected subset of mice (n=6 for SED and n=4 for HIIT).(8-9) See expanded methods section in the online supplement for further details, including antibodies and concentrations used. Briefly: We cut frozen sections of SOL at 7 μm thickness on a cryostat, mounting 3 SOL sections per slide. The sections were airdried for 1 hour, then rehydrated in phosphate buffered saline (PBS), each section circled with a hydrophobic PAP pen, then immersed in MoM (mouse on mouse blocker, Vector Labs), primary antibodies for 90 minutes at RT (room temperature), then secondary antibodies for 60 minutes at RT, followed by post-fixing in methanol (see **Table S1** for antibodies). PBS washes were used between steps. Coverslips were mounted using Vectashield antifade mounting medium (Vector Labs), and images taking on an EVOS fluorescent microscope at 200x total magnification. Data was quantified by blinded investigators using ImageJ.

Primary Antibody	Target	Supplier	Concentration	Secondary Antibody	Concentration
BA.D5 IgG2b mouse Concentrate[1]	**MHC1**	DHSB Iowa	1:100	Gt anti-Ms IgG2b, Alexa Fluor 647	1:500
SC.71 IgG1 , mouse supernatant[2]	**MHC2a**	DHSB Iowa	1:4	Gt anti-Ms IgG1, Alexa Fluor 488	1:250
BF.F3 IgM, mouse supernatant[3]	**MHC2b**	DHSB Iowa	1:4	Gt anti-Ms IgM, Alexa Fluor 555	1:250
Anit-laminin IgG Rabbit Polyclonal	**laminin**	Sigma #L9393	1:200	*Gt anti-Rb IgG, Alexa Fluor 350*	1:250

Table S1: Soleus IHC Antibodies. KEY: DHSB Iowa = Developmental Studies Hybridoma Bank

NOTES:

[1] The BA.D5 IgG2b developed by S. Schiaffino of the Universita degli Studi di Padova was obtained from the Developmental Studies Hybridoma Bank, created by the NICHD of the NIH, and maintained at The University of Iowa, Department of Biology, Iowa City, IA 52242.

[2]The SC.71 IgG1 mouse concentrate developed by S. Schiaffino of the Universita degli Studi di Padova was obtained from the Developmental Studies Hybridoma Bank, created by the NICHD of the NIH, and maintained at The University of Iowa, Department of Biology, Iowa City, IA 52242.

[3] The BF.F3 IgM developed by S. Schiaffino of the Universita degli Studi di Padova was obtained from the Developmental Studies Hybridoma Bank, created by the NICHD of the NIH, and maintained at The University of Iowa, Department of Biology, Iowa City, IA 52242.

Supplemental Results

In vivo Outcome Measures:

Physical Function: We measured physical function using the well-validated CFAB tests of rotarod, VWR, grip meter, inverted cling, and max speed test (treadmill), as well as x/y/z plane laser grid activity monitoring *(see* **Figure 2 Physical Function**). There were also many changes within groups from pre- to post-training paired t-tests), but fewer between groups (independent t-tests). A comprehensive breakdown of the statistical analysis can be found below and specifics in **Supplemental Dataset S1. Table 1** lists the more pertinent outcomes.

- Rotarod (overall motor function):
    - Within groups: rotarod time (SED: NC, no statistical change, numeric difference -14.1 ± %, p=0.373, Hedges' g 0.30; HIIT: +39.1% ± 14.9, *trend* p=0.078, Hedges' g 0.65).
    - Between groups: rotarod time (PRE: NC, p=0.528; Hedges' g 0.283, POST: NC, p=0.222; Hedges' g 0.61); rotarod percent change (NC, p=0.251, Hedges' g 0.59)
- VWR (volitional exercise):
    - Within groups: rotarod time (SED:-41% ± 25, p=0.004, Hedges' g 1.34; HIIT: -42% ± 23, *trend* p=0.002, Hedges' g 1.50).
    - Between groups: VWR meters per day (PRE: NC, p=0.528; Hedges' g 0.42; POST: *trend* p=0.097; Hedges' g 0.84); VWR percent change (NC, p=0.774, Hedges' g 0.148)
- Grip Meter (fore-limb strength):
    - Within groups: grip time (SED: -16% ± 4, p=0.007, Hedges' g 1.18; HIIT: NC, numeric +6% ± 12, p=0.838, Hedges' g 0.067); grip_mass (grip adjusted by multiplying with grams body mass) (SED: -35% ± 8, p=0.002, Hedges' g 1.56; HIIT: -NC. Numeric -14% ± 9, p=0.184, Hedges' g 0.65)
    - Between groups: grip time (PRE: NC, p=0.905; Hedges' g 0.424, POST: p=0.043; Hedges' g 1.05); grip time percent change (NC, p=0.126; Hedges' g 0.799); grip_mass (grip adjusted by body mass) (PRE: NC, p=0.822; Hedges' g 0.098, POST: *trend* p=0.053; Hedges' g 1.00); grip_mass percent change (PRE: trend *p=0.104*; Hedges' g 0.424, POST: p=0.043; Hedges' g 1.05)
- Inverted Cling (four limb strength/endurance):
    - Within groups: cling time (SED: -67% ± 6, p=0.004, Hedges' g 1.35; HIIT: -37% ± 10, p=0.025, Hedges' g 0.89); cling * mass (work) (SED: -64% ± 6, p=0.002, Hedges' g 0.49; HIIT: -14% ± 9, *trend* p=0.052, Hedges' g 0.46)
    - Between groups: cling time (PRE: NC, p=0.356; Hedges' g 0.16, POST: *trend* p=0.058; Hedges' g 0.1.00), cling * mass (PRE: NC, p=0.766, Hedges' g 0.283, POST: p=0.043, Hedges' g 1.05), cling time percent change (NC, p=0.126, Hedges' g 0.80); grip * mass percent change (SED -35%, HIIT -14%, *trend* p=0.104, Hedges' g 0.82)
- Treadmill (aerobic capacity, endurance):
    - Within groups: treadmill time (SED: NC, p=0.381, Hedges' g 0.30; HIIT: +71% ± 17, p=0.002, Hedges' g 1.56).
    - Between groups: treadmill time (PRE: p=0.528; Hedges' g 0.283, POST: p=0.028; Hedges' g 1.16); treadmill percent change (SED +6%, HIIT +71%, p=0.005, Hedges' g = 1.75)
- Activity Monitoring (activity rate):

- Within groups: total meters traveled per day (SED: NC, p=0.109, Hedges' g 0.58; HIIT: NC, p=0.881, Hedges' g 0.65).
- Between groups: total meters traveled per day (PRE: NC, p=0.393; Hedges' g 0.370, POST: p=0.739; Hedges' g 0.57)
-

Cognitive Function: We measured cognition using open field, NOR, y-maze, and puzzle-box *(see* **Figure 4** and **Supplemental Dataset S2 Cognitive Function** for more details). Differences in means within-groups were measured with paired t-test, and between groups were measured with Student's independent samples t-test.

- Open Field (exploratory behavior and anxiety):
  - Within groups multiple parameters changed pre- to post-intervention in both groups including: total distance traveled (SED: +75.0% ± 41.5, p=0.005, Hedges' g 0.52; HIIT: +89.3% ± 28, p<0.001, Hedges' g 1.36), average speed (SED: +74.6% ± 50.0, *trend* p=0.067, Hedges' g 0.53; HIIT: +90.1% ± 44.6, p<0.001, Hedges' g 1.36), maximum speed (SED: +23.6% ± 9.1, p=0.012, Hedges' g 0.53; HIIT: +50.6% ± 20.6, p=0.026, Hedges' g 0.79), time immobile defined as not moving for ≥ 10 seconds (percent change of overall mean pre- to post: SED: -88.6%, *trend* p=0.090, Hedges' g 0.56; HIIT: -89.9%, p=0.004, Hedges' g 1.21), and number of total immobile episodes (percent change of overall mean pre- to post: SED: -75%, *trend* p=0.052, Hedges' g 0.55; HIIT: -86.1%, p=0.001, Hedges' g 1.39). Anxiety was significantly reduced in HIIT, but not SED, reflected by increased time in center of field (SED: +97.8% ± 9.1, p=0.012, Hedges' g 0.49; HIIT: +50.6% ± 20.6, p=0.026, Hedges' g 1.03).
  - Between groups: There were no significant differences either before or after training.
- NOR (long-term memory):
  - Within groups: Multiple parameters changed pre- to post-intervention, including: total distance traveled (SED: +88.3% ± 34.1, p=0.005, Hedges' g 1.25; HIIT: +93.3% ± 41.3, p=0.006, Hedges' g 1.22), average speed (SED: +90.0% ± 34.5, p=0.005, Hedges' g 1.26; HIIT: +92.3% ± 40.2, p=0.006, Hedges' g 1.22), maximum speed (SED: +26.2% ± 3.9, p<0.001, Hedges' g 2.10; HIIT: +28.7% ± 6.2, p=0.006), time immobile (SED: -49.3% ± 8.8, p=0.016, Hedges' g 0.98; HIIT: -59% ± 14.0, p=0.007, Hedges' g 1.17), number of total immobile episodes (percent change of overall mean pre- to post: SED: +50.8%, p=0.004, Hedges' g 1.35; HIIT: -52.8%, p=0.014, Hedges' g 0.83). There was evidence for trends in changes from pre- to post-training to the investigation time of the novel object (NO) in both groups but there were no significant changes in familiar object (FO) investigation time: NO (SED: +50.8% ± 29.7, *trend p=0.053*, Hedges' g 0.73; HIIT: +300.4% ± 190.0, *trend p=0.096*, Hedges' g 0.53), FO (SED: +191% ± 119.2, p=0.11, Hedges' g 0.23; HIIT: +221.2% ± 149.9, p=0.822, Hedges' g 0.23); with obvious large individual variability. However, the major indicator of long-term memory, the discrimination index (measures the time spent investigating the familiar object versus time spent investigating the novel object) was not different between or within groups, either before or after, the intervention period.
  - Between groups: There were no significant differences pre- or post-intervention, in part due to large individual variability.

- Puzzle Box (executive function and memory):
  - Within groups: multiple parameters changed pre- to post-intervention including: PB1 (Puzzle Box parameter 1, the time to entry of escape trial on day1; SED: -45.2% ± 13.1, p=0.01, Hedges' g 1.1; HIIT: -68.3% ± 22.1, p=0.001, Hedges' g

1.6), PB2 (Puzzle Box parameter 2, the time to entry of escape trial on day 2; SED: no change, *NS* p=0.411 Hedges' g 0.27; HIIT: -93.1% ± 1.9, p=0.021, Hedges' g 0.93), PB1_2total (sum of Puzzle Box parameters 1 and 2; SED: -45.0% ± 12.1, p=0.015, Hedges' g 1.01; HIIT: -75.6% ± 4.3, p=0.004, Hedges' g 1.33), PB3.1 (time to entry of escape trial on day 3, measured from trial start; SED: -46.5% ± 16.1, p=0.043, Hedges' g 0.78; HIIT: -82.1% ± 5.5, p=0.005, Hedges' g 1.26), PB3.2 (time to clearing blockage to escape box on day 3, measured from trial start; SED: no change, p=0.144, Hedges' g 0.52; HIIT: -45.2% ± 12.5, p=0.011, Hedges' g 1.08), PB3_total (sum of PB3.1 and PB3.2 on day 3; SED: -28.5% ± 17.8, *trend* p=0.065, Hedges' g 0.69; HIIT: -60.0% ± 9.8, p=0.005, Hedges' g 1.25), and PBtotal (sum of PB1, PB2, PB3.1 and PB3.2; SED: -40.4% ± 13.3, p=0.021, Hedges' g 0.93; HIIT: -72.8% ± 3.0, p=0.002, Hedges' g 1.50).
    - Between groups: There were no significant differences pre-intervention. However, there were significant differences post-training found in PB1_2 percent change (p=0.032), PB3.1 percent change (*trend*, p=0.055), and in the overall major indicator of executive function PBtotal percent change (p=0.032), all of which demonstrated a greater effect in the HIIT group.

- Y-maze (spatial memory and exploratory behavior):
    - Within groups: Multiple parameters changed pre- to post-intervention including: total distance traveled (SED: no change, p=0.209, Hedges' g 0.44; HIIT: +45.6% ± 9.2, p=0.002, Hedges' g 1.94), average speed (SED: no change, p=0.217, Hedges' g 0.43; HIIT: +45.6% ± 9.3, p=0.002, Hedges' g 1.90), maximum speed (SED: +13.6% ± 5.7, *trend* p=0.064, Hedges' g 0.69; HIIT: +35.5% ± 4.3, p<0.001, Hedges' g 4.23), time immobile (SED: no change, p=0.179, Hedges' g 0.66; HIIT: -61.0% ± 7.5, p=0.011, Hedges' g 1.23), number of immobile episodes (SED: no change, p=0.487, Hedges' g 0.30; HIIT: -86.1%, p=0.003, Hedges' g 1.56), total arm entries (SED: +44.9% ± 14.5, p<0.001, Hedges' g 1.11; HIIT: +58.1% ± 5.4, p<0.001, Hedges' g 3.64), and number of spontaneous alternations (SA) defined as traveling subsequently into 3 different arms (e.g., AàBàC) without backtracking as a measure of spatial/short term memory (SED: +65.9% ± 2.8, *trend* p=0.077, Hedges' g 0.71; HIIT: +56.8% ± 2.8, p=0.001, Hedges' g 1.63). However, the major y-maze indicator percent of SA in relation to total arm entries did not change (Hedges' g: SED 0.33, HIIT 0.49), as both total number of entries and number of SA increased proportionally.
    - Between groups: There were no significant differences pre-intervention, other than related to average speed while traveling the maze (2.68 m/min in SED vs. 2.51 m/min in HIIT, p=0.080, Hedges' g: 0.89). There were no significant differences post-intervention other than percent change in maximum speed (+35.5% in HIIT versus +13.6% in SED, p=0.009, Hedges' g: 1.45) and percent change of immobile time (-61% in HIIT versus -30% in SED, *trend*, p=0.098, Hedges' g: 0.862), both demonstrating a stronger effect in HIIT.

Functional Composite Scores:

CFAB: Comprehensive functional assessment battery composite scoring system for physical function determined that HIIT preserved and SED lost functional capacity. ee **Figure 4**, **Table 3**, **Supplemental Results** section, and **Supplemental Dataset S1**.

- Within groups: CFAB (SED: Pre – Post = 4.52 ± 0.75, p<0.001, Hedges' g 0.30; HIIT: NC, numeric change Pre – Post = 0.77 ± 1.06, p=0.490, Hedges' g 0.41).

    - Between groups: no significant differences in CFAB (CFAB1 PRE: p=0.528; Hedges' g 0.283, CFAB2 POST: p=0.222; Hedges' g 0.61); but the changes in CFAB pre- to post were different: ΔCFAB (p=0.021; Hedges' g 1.23)
- CAB: Cognitive assessment battery composite scoring system determined that cognitive function was retained/improved with HIIT but not in SED. See **Supplemental Dataset S2.**
    - Within Groups CAB (SED: no change, p=0.921, Hedges' g 0.03; HIIT: +25%, p=0.022, Hedges' g 0.92).
    - Between groups: no significant differences in CAB raw scores (CAB1 PRE: p=0.391; Hedges' g 0.42, CAB2 POST: p=.240; Hedges' g 0.61); but the changes to CAB from pre- to post were different: ΔCAB (p=0.039; Hedges' g 1.08), CAB_percentchange (SED +1.99% versus HIIT +34.08%, p=0.067; Hedges' g 0.98).

Body Composition: See **Figure S3 Body Composition** and **Supplemental Dataset S4 Body Composition** for further details. We tracked body mass monthly during aging up to training and then weekly once training commenced. We measured fat percentage and total lean mass totals using EchoMRI, pre- and post-training.

- Within groups:
    - Body mass increased in both groups from pre- to post-training (SED: +9%, *trend* p=0.063, Hedges' g 0.69; HIIT: +12.8%, p=0.009, Hedges' g 1.12).
    - Fat mass (SED: NC, numerical +2.69 g ±1.57, p=0.110, Hedges' g 0.58; HIIT: +3.26 g ± 0.88, p<0.001, Hedges' g 1.16). However, SED fat mass post-training had a minor violation of normality (Shapiro-Wilk sig. = 0.032), and when the pre/post means were analyzed with the Wilcoxon Signed Rank test, fat mass was significantly increased (sig. = 0.017).
    - lean mass (SED: +0.95 g ± 0.23, p=0.005, Hedges' g 1.28; HIIT: +0.65 g ± 0.11, p<0.001, Hedges' g 1.87)
    - Fat percentage (SED: NC, numerical +5.1% ± 3.5, p=0.183, Hedges' g 1.11;. HIIT: +6.6% ± 1.7, p=0.006, Hedges' g 1.23).
- Between Groups: There were no significant changes between groups either pre- or post-training in body mass, lean mass, fat mass, or fat percentage.

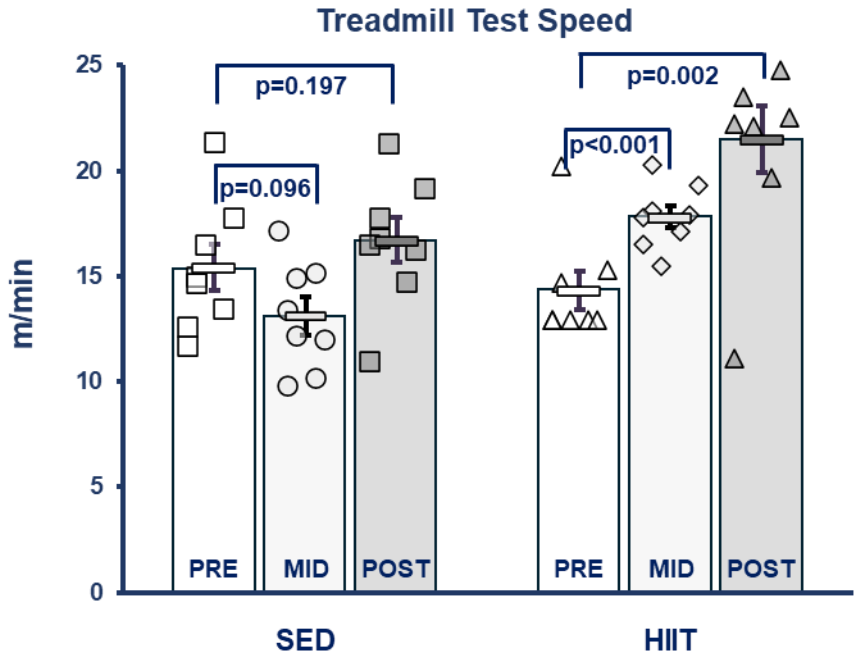

Figure S1 Treadmill Speed. A 2x3 (2 groups, SED and HIIT x three times, PRE, MID, and Post) mixed-model ANOVA showed with-in subject main effects of time ($F=17.07$, $p<0.001$, $\eta^2=0.549$) and the group*time interaction ($F=9.15$, $p<0.001$, $\eta^2=0.395$), and differences in means between subjects ($F=5.252$, $p=0.038$, $\eta^2=0.273$). Over the course of the training period the maximum treadmill speed of the SED mice did not significantly alter (paired t-test: pre->mid, $p=0.096$, Hedge's $g= 0.604$; pre->post, $p=0.222$, $g=0.448$), though there was a trend of a decline at midpoint. The HIIT mice had significant increases in maximum treadmill speed at both the midpoint (+18% at 7 weeks, $p<0.001$, $g=1.96$) and post-training (+26% at 14 weeks $p=0.002$, $g=1.56$) compared to the baseline pre-training speed. At baseline Sed and HIIT had no difference between groups ($p=0.470$, independent samples t-test), but HITT had faster times at both the midpoint (+36%, $p<0.001$, $g=2.11$) and the post-training tests (+29%, $p=0.028$, $g=1.56$), indicating positive aerobic capacity adaptations from training. KEY: SED=sedentary control group, HIIT=high intensity interval training group, PRE= before intervention period, MID=middle time point, POST=after intervention, squares/circles=SED, triangles/diamonds=HIIT, each symbol=speed of one mouse. Units are meters per minutes (m/min). The p-values in graph are from paired t-tests with pre. Significance is at $p<0.05$ and trends reported when $0.05<p<0.10$. Rectangles = means per group with standard error bars.

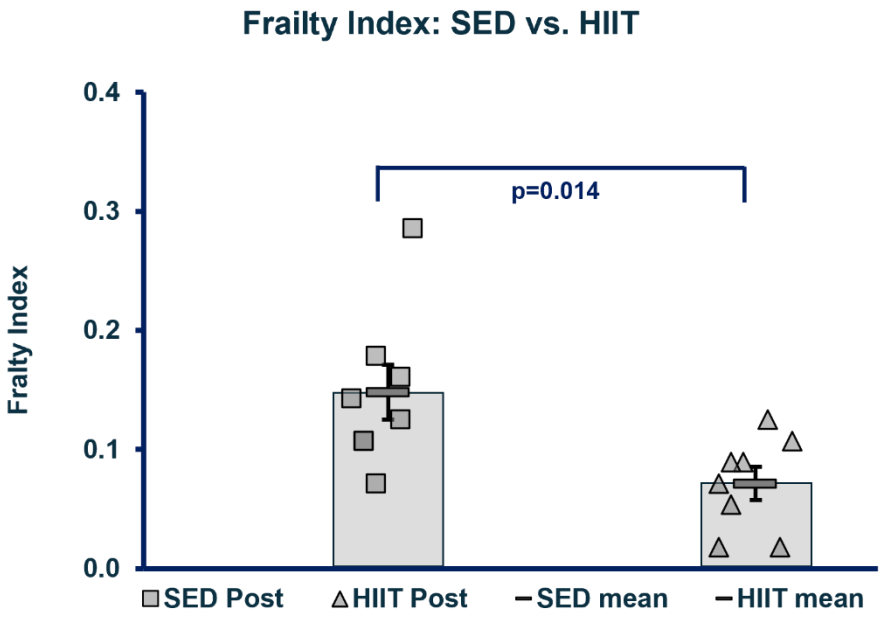

Figure S2 Frailty Index. HIIT significantly reduced the level of frailty measured by the frailty index. **KEY:** SED=sedentary control group, HIIT=high intensity interval training group, POST=after intervention, squares=SED, triangles=HIIT, each symbol=one mouse. The p-values in graph are from paired t-tests. Rectangles=means per group with standard error bars. Significance is at $p<0.05$ and trends reported when $0.05<p<0.10$, from independent samples t-test.

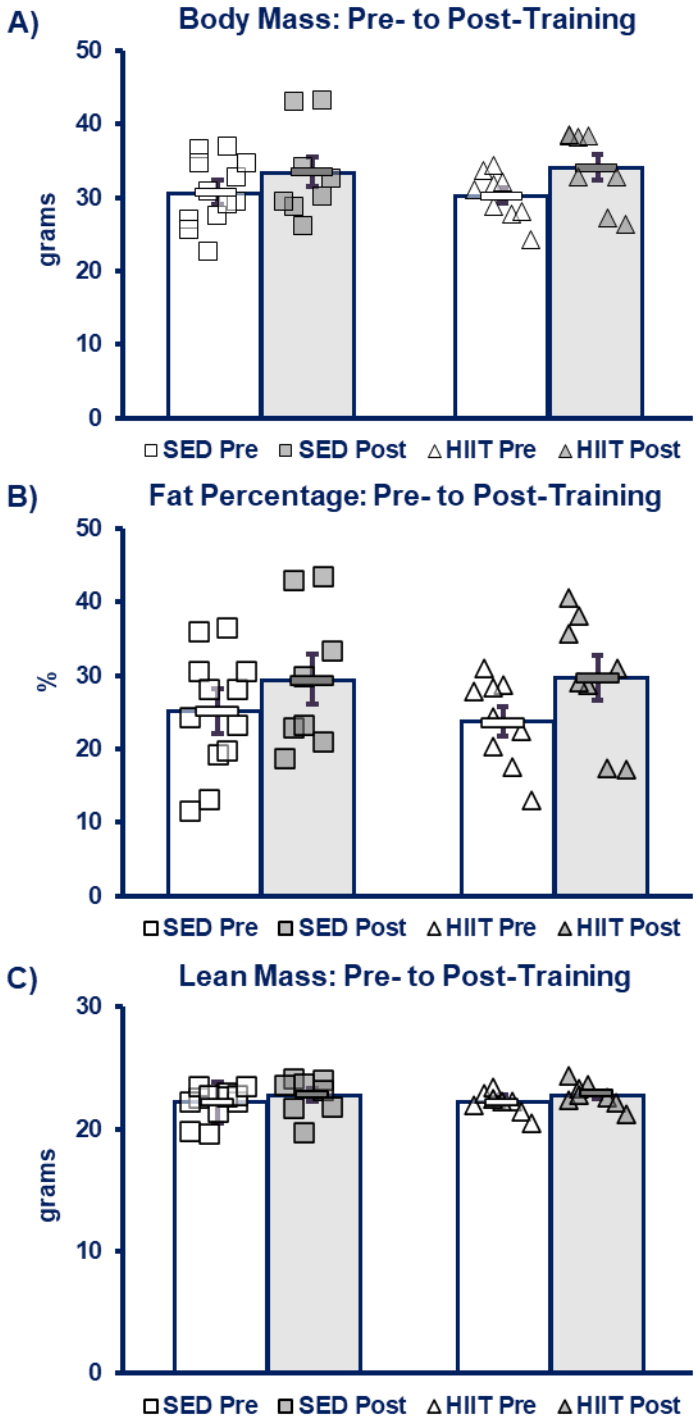

Figure S2 Body Composition. There were no differences between groups (independent samples t-test). **A) Body Mass. B) Fat Percentage. C) Lean Mass. KEY:** SED=sedentary control group, HIIT=high intensity interval training group, PRE=before intervention period, POST=after intervention, squares=SED, triangles=HIIT, open symbols=pre, shaded symbols=post, each symbol=one mouse. The p-values in graph are from paired t-tests. Rectangles = means per group with standard error bars. Significance is at $p<0.05$ and trends reported when $0.05<p<0.10$.

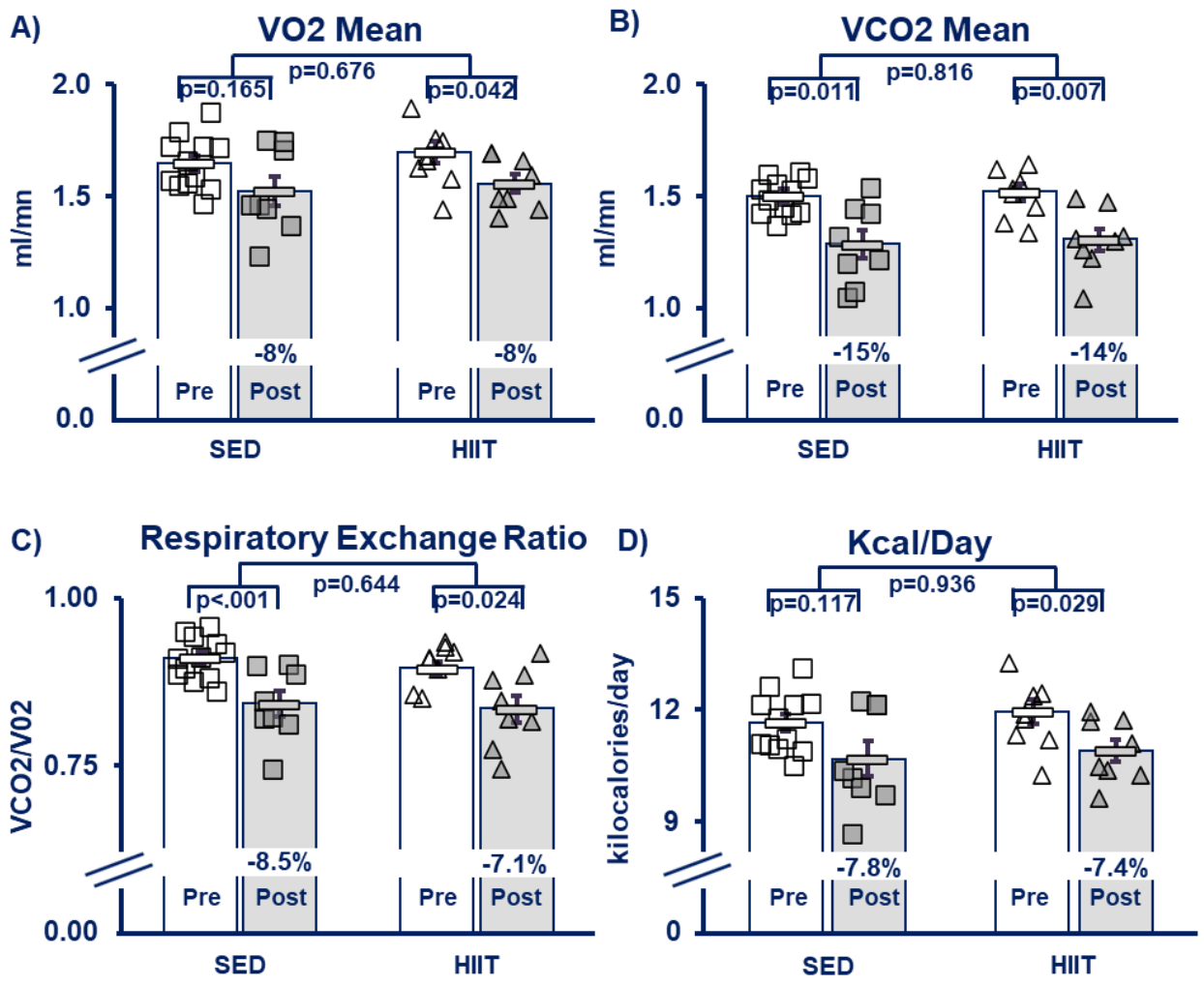

Figure S3 Metabolic Chamber Outcomes. A) VO2. Average oxygen consumption. **B) VCO2.** Average Carbon dioxide production. **C) Respiratory Exchange Ratio. D) Average kilocalories burned per day. KEY:** SED=sedentary control group, HIIT=high intensity interval training group, PRE= before intervention period, POST=after intervention, squares/circles=SED, triangles/diamonds=HIIT, each symbol=one mouse. The p-values in graph are from paired t-tests with pre. Significance is at $p<0.05$ and trends reported when $0.05<p<0.10$. Rectangles = means per group with standard error bars. Percentages in bar graphs = percent change from per- to post intervention

Supplemental References

1. Pajski ML, Byrd C, Nandigama N, Seguin E, Seguin A, Fennell A, et al. Endurance exercise preserves physical function in adult and older male C57BL/6 mice: high intensity interval training (HIIT) versus voluntary wheel running (VWR). Front Aging. 2024;5:1356954. doi:10.3389/fragi.2024.1356954 PubMed PMID: 38523671; PubMed Central PMCID: PMC10958787.

2. Pajski ML, Maroto R, Byrd C, Graber TG. Longitudinal Decline of Exercise Capacity in Male and Female Mice. J Gerontol A Biol Sci Med Sci. 2025 Feb 10;80(3):glae293. doi: 10.1093/gerona/glae293. PMID: 39693388; PMCID: PMC11809237.

3. Grilo GA, Cakir SN, Shaver PR, Iyer RP, Whitehead K, McClung JM, et al. Collagen matricryptin promotes cardiac function by mediating scar formation. Life Sci. 2023 May 15;321:121598. doi:10.1016/j.lfs.2023.121598 PubMed PMID: 36963720; PubMed Central PMCID: PMC10120348.

4. Armstrong AC, Gidding S, Gjesdal O, Wu C, Bluemke DA, Lima JAC. LV mass assessed by echocardiography and CMR, cardiovascular outcomes, and medical practice. JACC Cardiovasc Imaging. 2012 Aug;5(8):837–48. doi:10.1016/j.jcmg.2012.06.003 PubMed PMID: 22897998; PubMed Central PMCID: PMC3501209.

5. Lindsey ML, Kassiri Z, Virag JAI, de Castro Brás LE, Scherrer-Crosbie M. Guidelines for measuring cardiac physiology in mice. Am J Physiol Heart Circ Physiol. 2018 Apr 1;314(4):H733–52. doi:10.1152/ajpheart.00339.2017 PubMed PMID: 29351456; PubMed Central PMCID: PMC5966769.

6. Theobald D, de Castro Braz LE, Akula SM, Eells JB, Sriramula S. Inhibition of kinin B1 receptor alleviates SARS-CoV-2-induced long-lasting cardiovascular complications. Am J Physiol Heart Circ Physiol. 2025 Mar 1;328(3):H711–8.doi:10.1152/ajpheart.00861.2024 PubMed PMID: 39982452; PubMed Central PMCID: PMC12168569.

7. Theobald D, Nair AR, Sriramula S, Francis J. Cardiomyocyte-specific deletion of TLR4 attenuates angiotensin II-induced hypertension and cardiac remodeling. Front Cardiovasc Med. 2023;10:1074700. doi:10.3389/fcvm.2023.1074700 PubMed PMID: 37034342; PubMed Central PMCID: PMC10079917.

8. Graber TG, Fry CS, Brightwell CR, Moro T, Maroto R, Bhattarai N, et al. Skeletal muscle-specific knockout of DEP domain containing 5 protein increases mTORC1 signaling, muscle cell hypertrophy, and mitochondrial respiration. J Biol Chem. 2019 Mar 15;294(11):4091–102. doi:10.1074/jbc.RA118.005970 PubMed PMID: 30635399; PubMed Central PMCID: PMC6422100.

9. Graber TG, Rawls BL, Tian B, Durham WJ, Brightwell CR, Brasier AR, et al. Repetitive TLR3 activation in the lung induces skeletal muscle adaptations and cachexia. Exp Gerontol. 2018 Jun;106:88–100. doi:10.1016/j.exger.2018.02.002 PubMed PMID: 29452288; PubMed Central PMCID: PMC5911410.

Appendix A: Sample Frailty Index Form

Frailty Index Criteria Sheet

Group Date	Animal ID & FI Total									

Alopecia										
Loss of fur color										
Dermatitis										
Loss of whiskers										
Coat condition										
Tumours										
Distended abdomen										
Kyphosis										
Tail stiffening										
Gait disorders										
Tremor										
Body condition score										
Vestibular disturbance										
Hearing loss										
Cataracts										
Corneal opacity										
Eye discharge/swelling										
Microphthalmia										
Vision loss										
Menace reflex										
Nasal discharge										
Malocclusions										
Rectal prolapse										
Vaginal/uterine/penile prolapse										
Diarrhea										
Breathing rate/depth										
Mouse Grimace Scale										
Piloerection										